AGU PUBLICATIONS

JGR

Journal of Geophysical Research: Space Physics

RESEARCH ARTICLE

10.1002/2013JA018863

Key Points:
- HFAs occur at Venus at approximately the same rate as at the Earth
- They are relatively large and occur very close to the planet
- HFAs have a dominant role in the dynamics of the induced magnetosphere of Venus

Correspondence to:
G. A. Collinson,
glyn.a.collinson@nasa.gov

Citation:
Collinson, G. A., et al. (2014), A survey of hot flow anomalies at Venus, *J. Geophys. Res. Space Physics*, *119*, 978–991, doi:10.1002/2013JA018863.

Received 9 APR 2013
Accepted 14 DEC 2013
Accepted article online 19 DEC 2013
Published online 18 FEB 2014

A survey of hot flow anomalies at Venus

G. A. Collinson[1], D. G. Sibeck[1], A. Masters[2], N. Shane[3,4], T. L. Zhang[5], A. Fedorov[6], S. Barabash[7], A. J. Coates[3], T. E. Moore[1], J. A. Slavin[8], V. M. Uritsky[1,9], S. Boardsen[1,10], and M. Sarantos[1,10]

[1]Heliophysics Science Division, NASA Goddard Spaceflight Center, Greenbelt, Maryland, USA, [2]Institute of Space and Astronautical Science, JAXA, 3-1-1 Yoshinodai, Chuo-ku, Sagamihara, Kanagawa, Japan, [3]Mullard Space Science Laboratory, University College London, Holmbury St. Mary, Surrey, UK, [4]The Centre for Planetary Sciences at UCL/Birkbeck, London, UK, [5]Space Research Institute, Austrian Academy of Sciences, Graz, Austria, [6]Universite de Toulouse, UPS-OMP, IRAP, Toulouse, France, [7]Swedish Institute of Space Physics, Kiruna, Sweden, [8]Department of Atmospheric, Oceanic and Space Sciences, University of Michigan, Ann Arbor, Michigan, USA, [9]Institute for Astrophysics and Computational Sciences, Catholic University of America, Baltimore, Maryland, USA, [10]Goddard Planetary and Heliophysics Institute, University of Maryland, Baltimore County, Catonsville, Maryland, USA

Abstract We present the first survey of hot flow anomalies (HFAs) at the bow shock of Venus, expanding on our recent initial case study. A 3.06 sol (774 Earth day) survey of Venus Express magnetometer, ion spectrometer, and electron spectrometer data was undertaken in order to identify Cytherian HFAs. Seven events were discovered, corresponding to a statistical frequency $\approx 1.2 \pm 0.8$ per day, approximately the same rate as at the Earth. All seven HFAs were centered on a discontinuity in the solar wind, with inward pointing motional electric fields on at least one side, and exhibited electron and ion perturbations consistent with heating. For one event the calculation of continuous electron moments is possible, revealing that electron temperature increased from $\approx 2 \times 10^5$ K to 8×10^5 K in the HFA core (comparable to terrestrial and Kronian HFA observations), and density increased from ≈ 1 cm^{-3} to $\sim 2 \rightarrow 2.5$ cm^{-3} in the bounding compression regions. Cytherian HFAs were found to be physically smaller ($0.4 \rightarrow 1.7$ Venus radii (R_V)) than their terrestrial or Kronian counterparts, although are much larger when compared to the overall size of the system (≈130% of the subsolar bow shock distance), and occur very close ($1.5 \rightarrow 3.0\ R_V$) to the planet. Thus, we hypothesize that HFAs have a much more dominant role in the dynamics of the induced magnetosphere of Venus relative to the magnetospheres of magnetized planets.

1. Introduction

Hot flow anomalies (HFAs) are an explosive plasma phenomena found wherever there is an appropriate interaction between a current sheet and a collisionless shock, wherein a pocket of reflected solar wind plasma becomes heated and rapidly expands [*Schwartz et al.*, 1988]. They were first discovered by the *Active Magnetospheric Particle Tracer Explorer - UK Satellite* [*Schwartz et al.*, 1985] and by the *International Sun Earth Explorers* [*Thomsen et al.*, 1986]. Typical properties are as follows: (1) HFAs are centered on [*Schwartz*, 1995; *Eastwood et al.*, 2008] or found near to [*Omidi and Sibeck*, 2007; *Zhang et al.*, 2010] a discontinuity in the Interplanetary Magnetic Field (IMF) in close proximity to the Bow Shock [*Thomsen et al.*, 1988]. (2) A central core region of hot rarified plasma [*Paschmann et al.*, 1988], in which the magnetic field is noisy [*Tjulin et al.*, 2008], with an overall drop in the magnitude of the magnetic field ($|\mathbf{B}|$) [*Thomsen et al.*, 1986; *Lucek et al.*, 2004; *Koval et al.*, 2005]. (3) Bounding compressive/mildly shocked regions of denser heated plasma associated with peaks in $|\mathbf{B}|$ [*Onsager et al.*, 1990; *Thomas et al.*, 1991]. (4) An overall deflection in solar wind flow [*Facskó et al.*, 2009; *Masters et al.*, 2009].

HFAs are important at the Earth because they are common (≈3 per day [*Schwartz et al.*, 2000], ≈2 per day [*Facskó et al.*, 2009]), and can cause global effects on the magnetosphere and ionosphere [*Sibeck et al.*, 1998, 1999]. The large fluctuations in pressure associated with an HFA drive large outward motions in the location of the magnetopause, resulting in measurable deflections in ground based magnetometers [*Eastwood et al.* 2008]. This motion drives currents throughout the magnetosphere, precipitating particles into the ionosphere resulting in auroral brightenings [*Sibeck et al.*, 1999].

HFAs are thought to form as a result of shock reflected solar wind ions being focused onto the IMF discontinuity through motional electric fields [*Thomsen et al.*, 1988; *Burgess*, 1989; *Thomsen et al.*, 1993; *Omidi and Sibeck*, 2007]. Thus, an important requirement for HFA formation is thought to be motional electric fields

pointing into the discontinuity on at least one size [*Schwartz et al.*, 2000], although this is not always the case [*Schwartz et al.*, 2000; *Wang et al.*, 2013]. The exact mechanism for plasma heating is currently unclear. *Gary* [1991] postulated that ions are heated through ion-ion instabilities, whilst recently *Zhang et al.* [2010] suggested that electron heating may be a result of hybrid waves. More recently, a new class of HFA-like phenomena has been reported in both hybrid simulations [*Omidi et al.*, 2013], and *Time History of Events and Macroscale Interactions during Substorms* (THEMIS) observations [*Zhang et al.*, 2013]. These so called "spontaneous hot flow anomalies" are thought to form as a result of foreshock cavitons interacting with the bow shock, without the need for a tangential discontinuity. However, this study only considers "classic" HFAs which form as a result of the interaction between a solar wind discontinuity and a standing planetary bow shock. Following their initial discovery at Earth, HFAs have subsequently been observed at Saturn [*Masters et al.*, 2008, 2009] and at Mars [*Øieroset et al.*, 2001] (although no ion perturbations could be observed in this case, since *Mars Global Surveyor* carried only an electron spectrometer).

Recently, [*Collinson et al.*, 2012a] reported the observation of an HFA in the foreshock of the planet Venus, following up on an HFA-like magnetic signature observed by the Mercury-bound NASA *Mercury Surface, Space Environment, Geochemistry and Ranging* (MESSENGER) spacecraft [*Slavin et al.*, 2009]. *Collinson et al.* [2012a] used both field and particle measurements from the *Venus Express* [*Svedhem et al.*, 2007] Magnetometer [*Zhang et al.*, 2006] and the Analyzer of Space Plasmas and Energetic Atoms (ASPERA) [*Barabash et al.*, 2007] to unambiguously demonstrate the occurrence of HFAs in the Cytherian foreshock. The properties of this Cytherian HFA were consistent with those described above, and within the limitations of the data set, appeared consistent with HFAs observed at other planets throughout the solar system.

While *Collinson et al.* [2012a] was able to confirm their occurrence, the paper was only a single case study and thus was unable to comment on whether or not the observed event was typical, nor was it able to comment on the general properties of Cytherian HFAs. Whilst heating was demonstrated in the compression regions of the HFA, *Collinson et al.* [2012a] was unable to demonstrate the expected temperature increase in the core, and was only able to speculate on changes in electron density. This was believed this to be due to a data gap, the short timescale of the event, the low plasma flux in the region, and the low geometric factor [*Collinson et al.*, 2012b] (sensitivity) of the *Venus Express* ASPERA Electron Spectrometer (ASPERA-ELS) due to errors during manufacture [*Collinson et al.*, 2009].

In this paper we present our extension of the work of *Collinson et al.* [2012a] through a 3.06 Venus Solar day (3.06 sol, 774 Earth days) *Venus Express* campaign to determine the typical properties of Cytherian Hot Flow Anomalies so that they can be compared against their terrestrial and Kronian counterparts. Additionally, we present evidence for the expected increases in plasma temperature and density in order to further confirm their presence at Venus.

This paper is organized as follows. In section 2, we outline our survey and the criteria used for event selection. In section 3 we present full data sets from our best example of a Cytherian HFA which occurred on 26 February 2009, from which we were able to extract electron moments to demonstrate the expected heating in the core, and density enhancements in the bounding compression regions. In section 4 we calculate and compare the general properties of Cytherian HFAs to their terrestrial and Kronian counterparts. The properties discussed are solar wind velocity during formation, frequency, size, observed direction of motional electric fields, and speed along the bow shock. Finally, in section 5, we summarize our findings.

2. A Survey of Cytherian Hot Flow Anomalies

This survey used data from three instruments: The *Venus Express* Magnetometer (MAG) [*Zhang et al.*, 2006]; Analyser of Space Plasmas and Energetic Atoms (ASPERA) Electron Spectrometer (ELS); and ASPERA Ion Mass Analyzer (IMA) [*Barabash et al.*, 2007]. A brief description of each, together with their limitations in measuring Cytherian foreshock phenomena can be found in *Collinson et al.* [2012a, section 2]. The *Venus Express* is in an elliptical quasi polar orbit with a period of ~24 hours [*Titov et al.*, 2006], and spends only ~10 min out of each orbit in the Cytherian foreshock, the region in which this investigation was focused. Therefore, in order to obtain a reasonable chance of finding events, this necessitated a prolonged 3.06 sol observation campaign of 744 orbits from 2008 and 2009. In order to match the rigour of *Collinson et al.* [2012a], we required that a combination of field, electron, and ion measurements be available in order to confidently identify HFAs from the plethora of other foreshock phenomena. Therefore, 129 orbits were rejected because data from one or all of our three instruments were not available.

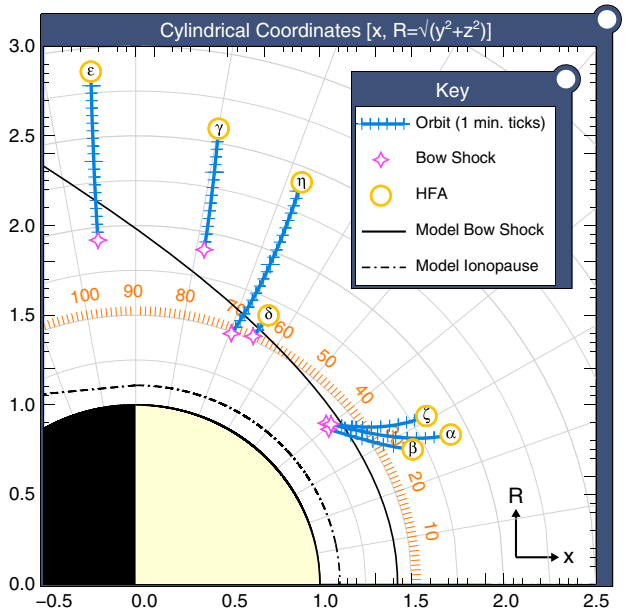

Figure 1. Map showing the positions of hot flow anomalies at Venus in VSO cylindrical coordinates relative to an idealized *Slavin et al.* [1980] bow shock. Units are in Venus radii.

For the remaining 615 orbits (2.53 sol), we monitored the ~30 min upstream of the Cytherian foreshock for events with all three following characteristics: (1) A sudden change in magnetic field orientation that might be associated with a solar wind discontinuity. (2) A perturbation in the ASPERA ELS electron spectra which might indicate an increase in flux or temperature. (3) A perturbation in the ASPERA-IMA ion spectra.

Our search uncovered seven candidate events (including HFA β, published in *Collinson et al.* [2012a]) and several other dynamic foreshock phenomena, including the first observation of Short Large Amplitude Magnetic Structures at Venus (SLAMS) [*Collinson et al.*, 2012c]. Each HFA candidate was given a Greek identifying character in chronological order ($\alpha \rightarrow \eta$). Figure 1 shows a scale map of their positions relative to the planet and an idealized bow shock according to *Slavin et al.* [1980]. The coordinate system used in this paper is Venus Solar Orbital (VSO), where x points toward the Sun, y backward along the orbital plane of Venus, and z completes the right hand set upward out of the plane of the ecliptic. In plotting Figure 1, we have taken 3-D positions in VSO and collapsed them into a special cylindrical 2-D co-ordinate system, where the x axis points toward the Sun (as in VSO), and the y axis is the radius from the Venus/Sun line, $R = \sqrt{(y^2 + z^2)}$. This is so that the relative positions and distances of each event from the bow shock can be more clearly plotted in two dimensions. The units are Venus Radii (R_V), where we have taken 1 R_V = 6052 km.

HFA candidates are denoted in Figure 1 by a labelled gold circle, and the actual position of the corresponding bow shock crossing by pink stars, although with an average 14 min time difference between HFA and bow shock encounter, it is quite possible that the bow shock was not in the location shown in Figure 1 during the HFA, especially given that HFAs are known to drive large-scale motions in the Earth's magnetosphere [*Sibeck et al.*, 1999; *Eastwood et al.*, 2008]. Each event is linked to its companion bow shock crossing by a blue line, which is a plot of the orbital track of the *Venus Express*, with tick marks plotted at 1 min intervals. As can be seen, HFA candidates were discovered throughout the foreshock. It is important to note that although no events are shown within ~25° of the subsolar point (see angles marked on Figure 1), this is because the *Venus Express* does not have access to these regions due to the nature of its orbit.

The further that *Venus Express* explored into the flanks, the further from the nominal position of the bow shock it was possible to observe an HFA. Those discovered toward the subsolar point (α, β, and ζ) were all within ≈10 min of the bow shock crossing, whereas in the flanks, events were discovered up to ≈20 min away from a bow shock crossing. With the exception of event δ, flank HFAs were all further away from both the observed bow shock position, and from the statistical nominal bow shock position [*Slavin et al.* 1980].

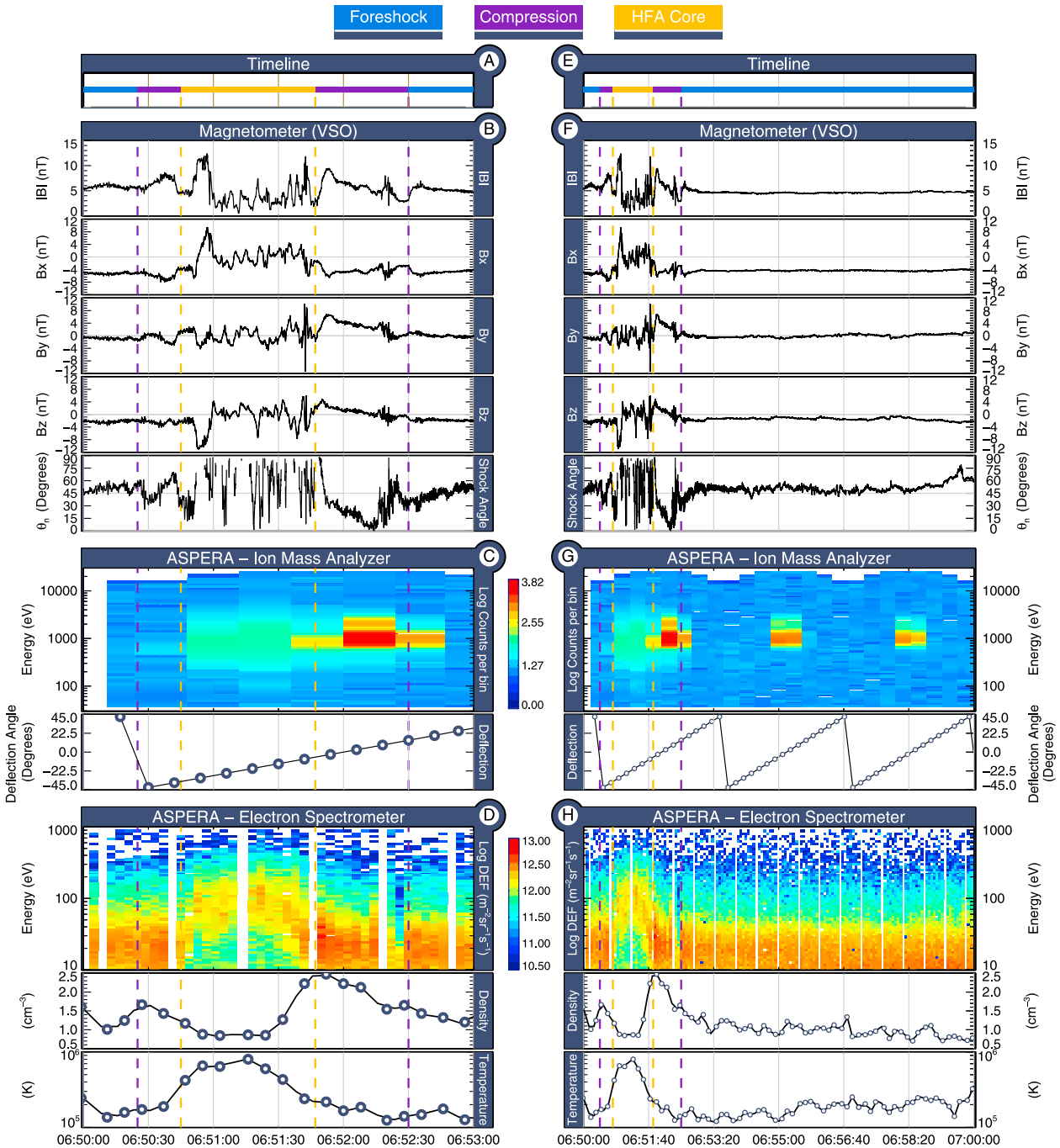

Figure 2. Hot flow anomaly ζ as observed by the ESA *Venus Express* on the 26 February 2009. (a–d) The period from 06:50:00 to 06:53:00 Greenwich Mean Time. (e–h) The period from 06:50:00 to 07:00:00 Greenwich Mean Time so that the field and particle perturbations of HFA ζ can be more easily contrasted against normal solar wind conditions.

We posit that the reason for this is most likely due to the geometry of the foreshock, wherein (depending on solar wind conditions) it is possible for the foreshock to extend farther from the bow shock on the flanks than at the subsolar point [*e.g., Eastwood et al.,* 2005, and references therein]. In addition, the presence of magnetic wave activity on at least one side of each event, consistent with foreshock waves, leads us to conclude that all of our HFA candidate events must have magnetic connection to the bow shock on at least one side. Thus, we conclude that all Cytherian HFA candidates were found in or on the edge of the foreshock, as is the case at the Earth [*Schwartz et al.*, 2000].

3. Hot Flow Anomaly Zeta (ζ)—26 February 2009

Collinson et al. [2012a] established the existence of HFAs at Venus and presented a single case study of the best example at the time. However, it was not possible to extract continuous plasma moments throughout that event. In this section, we present a better example of a Cytherean HFA (Zeta - ζ) and use measurements of the unique electron signature within the event to extract bulk electron temperature and density. Thus, as further confirmation that these events are HFAs, we demonstrate the expected temperature increase in the core, and density increases in the bounding compression regions.

Figure 2 shows event ζ as observed by *Venus Express* on 26 February 2009. Figures 2a–2d cover the period from 06:50:00 to 06:53:00 Greenwich Mean Time. Figures 2e–2h cover the period from 06:50:00 to 07:00:00 Greenwich Mean Time so that the field and particle perturbations of event ζ can be more easily contrasted against normal solar wind conditions. Figures 2a and 2e show a color coded timeline of the event. Periods when *Venus Express* was in the foreshock are blue, the core of the HFA in gold, and the bounding compression regions in purple; Figures 2b and 2f show magnetometer data at 32 samples per second. Each component is plotted separately with θ_n, the angle that the magnetic field vector makes with the normal to the bow shock of Venus (using the *Slavin et al.* [1980] bow shock model), plotted beneath; Figures 2c and 2g show data from ASPERA-IMA, with time/energy spectrogram on top, and corresponding electrostatic deflection angle [*Barabash et al.*, 2007; *Collinson et al.*, 2012a] plotted beneath; Finally, Figures 2d and 2h show data from ASPERA-ELS, with spectrogram on top, and corresponding density and temperature plotted beneath. We shall now examine the measurements made by each of these three instruments in turn.

3.1. Magnetometer

Figure 2b shows observations made at 32 samples per second by the *Venus Express* Magnetometer (MAG). There is a clear change in the orientation of the IMF from 06:50 to ~06:52, largely evident in a change in *By* from 0 to around +4 nT. The bottom panel shows a plot of the angle (θ_n) that the magnetic field makes with the bow shock of Venus, and exhibits a deflection of approximately 30°, consistent with the presence of a discontinuity in the solar wind. Interestingly, after ~06:52:15, the IMF rotates back to its original orientation, and is the only event which does not exhibit a lasting change in IMF orientation before and after. Given that the presence of a tangential discontinuity is a known formation requirement for HFAs, we speculate that whilst a discontinuity was present, *Venus Express* only briefly encountered it.

As with event β that was published in [*Collinson et al.*, 2012a], event ζ exhibits a magnetic signature with all the main features of an HFA. Within the core of the event, $|\mathbf{B}|$ drops from ≈5 nT in the foreshock to close to zero. On either side of the core the field strength is enhanced from 5 nT in the surrounding foreshock, to 8→9 nT. We attribute these magnetic signatures to a weakly shocked plasma that is being compressed as the HFA rapidly expands into the solar wind.

3.2. Ion Mass Analyzer

Ion observations of Cytherean HFAs are limited by the 192*s* temporal resolution of IMA, corresponding to the period required for the electrostatic deflector plates to scan through $-45° \Rightarrow +45°$ of elevation. This is longer than the ~55s required for *Venus Express* to cross through the core region of event ζ, meaning that extracting reliable ion moments would be very challenging. However, we are still able to present evidence for the expected deflection in ion flow.

Figures 2c and 2g show data from the ASPERA Ion Mass Analyzer (IMA), with time/energy spectrogram on top (units of log counts per bin), and electrostatic deflection angle plotted beneath. Note that IMA was operating in a mode wherein counts from neighboring deflection states were summed in order to reduce the amount of data telemetered back to Earth. The solar wind ion population (most easily seen in Figure 2g) appears regularly between deflection angles of −5° and 22.5°, centered on a deflection angle of ~5° and an energy of ~1 keV.

A new population of ions appears during the core of event ζ, centered at ~1000 eV, spanning the two time bins between ~06:50:50 and ~06:51:40. As these time bins correspond to approximately −30° to −10° electrostatic deflection angles, these ions are therefore coming from a different direction than those in the Solar Wind. Since this population is not observed at any other time in the Solar Wind on this day, as with HFA β, we assert this to be qualitatively consistent with that of a deflection in plasma flow associated with an HFA. Whilst we only present IMA data for event ζ, this signature ion perturbation was observed for each

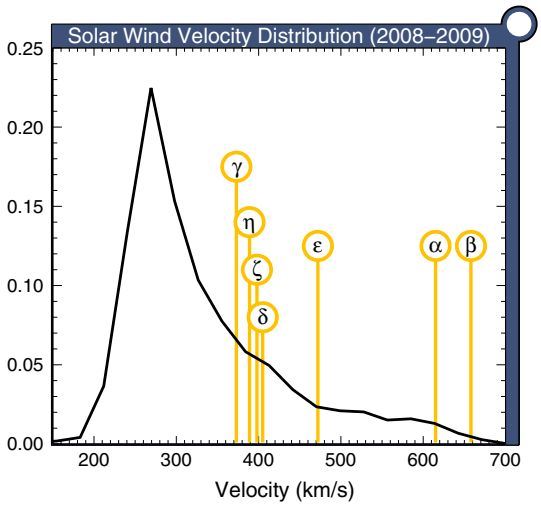

Figure 3. Probability distribution of peak of solar wind bulk velocity from 2008 to 2009, covering the HFA observation campaign. The bulk velocity during each of the HFAs is shown in gold.

of the seven events presented in this paper and is one of the contributing pieces of evidence that led us to conclude that they are also Cytherean HFAs.

3.3. Electron Spectrometer

HFA ζ features a population of energetic ($\approx$100 eV) electrons at flux levels sufficient to extract continuous moments. This population, unique amongst the Cytherean HFAs presented here, is qualitatively similar to those previously published for HFAs at Earth [*Zhang et al.*, 2010], Mars [*Øieroset et al.*, 2001], and Saturn [*Masters et al.*, 2009].

Figures 2d and 2h show measurements by the ASPERA Electron Spectrometer (ELS), with a time/energy spectrogram on top (in units of log differential energy flux), with density and temperature plotted below. White vertical bars in the spectrograms are data gaps. ELS has a very limited field of view, and thus, these should be regarded as pseudo-moments where isotropy has been assumed. Additionally, these data products have been processed by removing background counts and spacecraft photoelectrons, and then smoothed (by averaging every two energy sweeps) to improve counting statistics, so that the overall bulk changes can be more easily observed.

By comparison to the solar wind, the electrons within the core of the events are distinctly energized. The peak of the distribution increases from $\sim$20 eV in the solar wind, to $\sim$100 eV in the core (note that the spacecraft potential is approximately 10 eV). Like event β, there is enhanced flux in the compression regions, which *Collinson et al.* [2012a] suggested was consistent with the expected increase in plasma density. Analysis of event ζ confirms this hypothesis, with increases from $\approx$1 cm^{-3} to 1.7 cm^{-3} in the first compression region and $\approx$2.5 cm^{-3} in the second compression region. Furthermore, we are now able to demonstrate the expected electron heating in the core of a Cytherian HFA, with an increase in temperature from $\approx 2 \times 10^5 K$ to $8 \times 10^5 K$ in the HFA core, which is comparable to terrestrial and Kronian HFAs.

This energized electron spectra is unique to event ζ, with all other events presented in this paper having the same signature as that presented in *Collinson et al.* [2012a] (and therefore not shown for the sake of brevity). At present, we can only speculate on why event ζ has this electron population. It is possible that ζ may represent a more developed example, and this is a signature of a more mature HFA. Alternatively, given that event ζ was observed very close to the bow shock, perhaps this population is due to shock-reflected electrons, or other such localized phenomena which can only be seen when in close proximity to the bow shock.

4. General Properties of Cytherian Hot Flow Anomalies

4.1. Solar Wind Velocity During HFA Formation

Figure 3.2 shows a normalized histogram of the peak bulk solar wind velocity at Venus as measured by ASPERA-IMA over 2008–2009 (the period of the HFA survey). The velocity of the solar wind during each of the 7 HFAs is overplotted in gold, and also shown in the fifth column of Table 2. In all cases, we observe that the solar wind velocity was higher than the mode of $\sim$275 km/s, and no HFAs were observed when the solar wind was slower than 370 km/s. Additionally, whilst solar wind velocities greater than 600 km/s make up only 3% of all solar wind measurements during 2008–2009, two of the HFAs (α, and β) were observed during these exceptionally fast and rare solar wind conditions. These observations are consistent with the conclusions of *Facskó et al.* [2009, 2010], who reported that an apparent formation condition for HFAs at Earth is that the solar wind velocity must be faster than average by $\approx$100 $\Rightarrow$ 200 km/s.

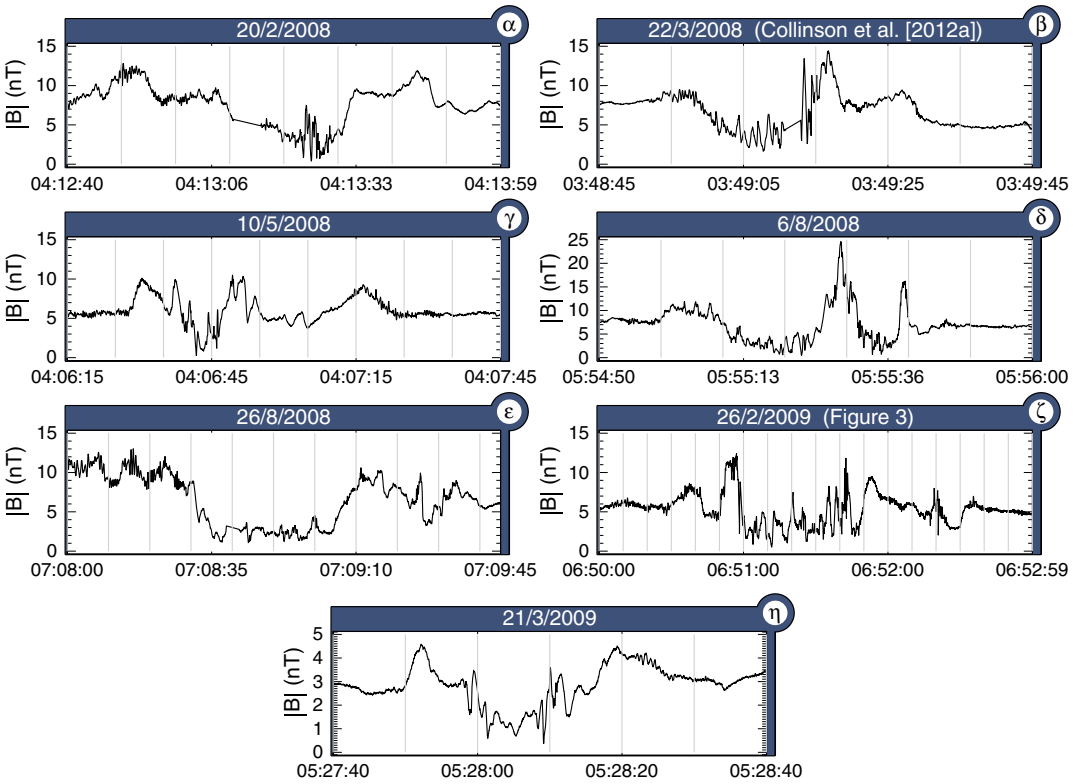

Figure 4. Magnetic magnitude for all seven Cytherian hot flow anomalies, with vertical grey lines at 10 s intervals so that relative durations can be compared.

4.2. Frequency of Occurrence

Based on 30 events, *Schwartz et al.* [2000] calculated that HFAs occur at Earth at a rate of ≈3 HFAs per day. More recently *Facskó et al.*, [2009] (a survey of 124 HFAs over 3 years) reported a rate of $\approx 2d^{-1}$, or specifically $2.2 \pm 1.2d^{-1}$ in 2003, $2.5 \pm 1.5d^{-1}$ in 2006, and $2.1 \pm 1.5d^{-1}$ in 2007. At Venus, seven HFAs were found in 615 orbits (1 orbit taking ≈24 hours). However, it does not follow that HFAs only occur at Venus once every hundred days. This is because, out of the ∼24 hours orbit, the *Venus Express* only spends a few minutes in the foreshock. Thus, in order to make a first approximation for the frequency of HFAs at Venus, we must first estimate how much time (out of the 2.53 sols of usable data) was spent monitoring the region where there is even a theoretical possibility of encountering an HFA.

The period between bow shock crossing and HFA encounter was highly variable, being as brief as 3 min and 16 s (3:16) for HFA δ, to 23 min and 2 s (23:02) for HFA η. However, on average, the HFAs were observed within 14 min of the bow shock (with a standard deviation of 7.5 min). Thus, for a rough first-order approximation of the frequency of Cytherian HFAs, let us assume that the *Venus Express* has only a 14 min window of observation per orbit (Note that although there are two bow shock crossings per orbit, inbound and outbound, typically only the upstream crossing was examined unless the orbit was close to the flanks). Therefore, the total time spent in this region was approximately ≈5.98 Earth days (615 orbits × 14 min). Seven HFAs equates to 0.85 days per HFA, or $\approx 1.2 \pm 0.8$ HFAs per day.

However, if it is assumed that, as for Earth, a minimum solar wind velocity is required for HFA formation [*Facskó et al.*, 2009, 2010], then this must also be taken into account. Given that all seven HFAs were observed when the velocity of the solar wind at Venus was faster than 370 km/s, let us assume this to be the minimum threshold required for Cytherian HFA formation. Using this as a lower limit of integration of the velocity distribution function shown in Figure 3.2, we find that solar wind velocities above 370 km/s were only encountered 28% of the time. Thus, even though *Venus Express* spent ≈5.98 Earth days in the region where it is possible to observe an HFA, on average the solar wind may only have been fast enough to generate one 28% of the time. If this assumption is made, then the total period of observation when it was

Table 1. Average Magnetic Conditions Before ($\hat{\mathbf{B}}_{pre}$) and After ($\hat{\mathbf{B}}_{post}$) the Cytherian HFAs, Showing Change in Mean Field Direction ($\Delta\theta_{\mathbf{B}}$), the Change in Angle Which the Corresponding Current Sheet Makes With the Bow Shock Normal ($\Delta\theta_n$), and the Angle Between the Current Sheet Normal and the Sun-Venus Axis ($\theta_{\hat{\mathbf{n}}.\hat{\mathbf{x}}}$)

	$\hat{\mathbf{B}}_{pre}$			$\hat{\mathbf{B}}_{post}$			$\Delta\theta_{\mathbf{B}}$	$\Delta\theta_n$	$\theta_{\hat{\mathbf{n}}.\hat{\mathbf{x}}}$
Event	$\hat{B}_x$	$\hat{B}_y$	$\hat{B}_z$	$\hat{B}_x$	$\hat{B}_y$	$\hat{B}_z$	(°)	(°)	(°)
α	−0.9	−0.34	0.25	−0.91	0.35	0.23	41	30.8	91
β	−0.73	−0.49	−0.47	−0.59	0.44	−0.69	42	31.8	20
γ	−0.7	−0.05	0.71	−0.73	−0.51	−0.45	77	1.57	67
δ	0.67	0.57	−0.48	0	0.73	−0.68	42	33.8	93
ϵ	0.83	−0.23	0.5	−0.8	0.53	0.3	129	90.7	115
ζ	−0.91	−0.14	−0.38	−0.96	0.23	−0.18	24	15.2	74
η	−0.83	0.36	−0.41	−0.54	0.7	−0.47	26	2.7	74

theoretically possible for *Venus Express* to encounter an HFA was ≈1.7 Earth days. Under this regime, then the frequency of HFAs at Venus is described by the expression below.

$$Frequency = \begin{cases} 4.2 \pm 2.7d^{-1} & \text{if } (V_{sw} > 370 \text{ km/s}) \\ 0 & \text{otherwise} \end{cases}$$

4.3. Magnetic Observations

Figure 4 shows a plot of the variations in the magnitude of the magnetic field strength ($|\mathbf{B}|$) during each event. Whilst there is a good degree of variability between each, all have the same overall signature as events β and ζ. First, each exhibits a drop in field strength below ambient solar wind values and magnetic pulsations in the core. Second, each is bounded by a pair of magnetic field strength enhancements associated with the bounding compressive regions. An exception to this is event delta (δ), which on first glance appears to be a "double" HFA, with two distinct cores separated by a large spike in field strength to ∼25 nT. We speculate that the most likely explanation is a double *encounter* with a single HFA, much in the same way that *Venus Express* can make multiple "early" bow shock crossings in a single orbit [e.g., *Collinson et al.*, 2012c]. This overall HFA signature is very similar to those observed at Earth [*Thomsen et al.*, 1986; *Lucek et al.*, 2004] *(etc)*, Saturn [*Masters et al.*, 2008, 2009], Mars *Øieroset et al.* [2001], and that observed at Venus by MESSENGER [*Slavin et al.*, 2009].

Each event is associated with an abrupt change in the magnetic field orientation across each event, consistent with a discontinuity in the IMF. The mean unit vector of the field direction before ($\hat{\mathbf{B}}_{pre}$) and after ($\hat{\mathbf{B}}_{pre}$) the HFA is shown in the second and third columns of Table 1. The corresponding change in magnetic field direction for the seven events $\Delta\theta_{\mathbf{B}}$ is shown in the fourth column of Table 1. The average change in field direction was 54°, not inconsistent (given there are only seven events) with the average change reported at Earth of between 60° [*Facskó et al.*, 2008] and 70° [*Schwartz*, 1995; *Facskó et al.*, 2010]. Theory predicts that the events occur at the intersection of tangential discontinuities with the bow shock. Assuming this to be the case, we calculated normals to the discontinuities ($\hat{\mathbf{n}}$) using equation (2) after *Hudson* [1970].

$$\mathbf{n}_{cs} \equiv \bar{\mathbf{B}}_{pre} \times \bar{\mathbf{B}}_{post} \quad (1)$$

$$\mathbf{n}_{cs} = n\hat{\mathbf{n}} \quad (2)$$

where $\bar{\mathbf{B}}_{pre}$ is the average magnetic field vector before and $\bar{\mathbf{B}}_{post}$ the average field after. As with *Collinson et al.*, [2012b], knowing $\hat{\mathbf{n}}$, we assumed the discontinuity to be a flat plane, and using geometry determined whether it intersected with a nominal bow shock as described by *Slavin et al.* [1980]. Thus, we were able to determine that in all cases that the underlying discontinuity was in contact with the bow shock, a key requirement for HFA formation.

Another known requirement for HFA formation is that the current sheet must be oriented to lie roughly parallel to the Sun-Venus line. This is so that there is sufficient time for the current sheet to interact with the bow shock and for the HFA to form before the current sheet is swept off into interplanetary space by the advection of the solar wind. Thus, in the VSO co-ordinate system, $\hat{\mathbf{n}}$ should be roughly perpendicular to $\hat{\mathbf{x}}$.

Table 2. Properties of Known Cytherian HFAs[a]

Event	Date (dd/mm/yyyy)	Duration (≈ s)	Cross Section (km)	Cross Section (R_V)	$\|V\|_{sw}$ (km/s)	**E** Field Toward Current Sheet?	Speed Ratio (Before)	Speed Ratio (After)	$\theta_{CS.BS}$ (deg)
α	20/2/2008	26	4,345	0.7	**615**	Both sides	0.32	0.17	106
β	22/3/2008	19	4,411	0.7	**658**	Both sides	0.31	0.48	69
γ	10/5/2008	19	2,433	0.4	373	Both sides	0.22	0.21	70
δ	6/8/2008	38	3,531	0.6	405	Before	0.12	0.14	103
ϵ	26/8/2008	41	3,874	0.6	472	Both sides	**1.36**	**3.11**	102
ζ	26/2/2009	**55**	**10,360**	**1.7**	398	Before	0.33	0.45	62
η	21/3/2009	27	5,688	0.9	389	After	0.47	0.49	57

[a]Important outliers discussed in this study are in bold.

The right hand most column of Table 1 shows the angle ($\theta_{\hat{\mathbf{n}}.\hat{\mathbf{x}}}$) between the current sheet normal and the *x* axis. In all cases, the value calculated was close to 90° (the mean is 81° ± 21°), which is in agreement with this known formation requirement for HFAs.

4.4. Duration and Size

Using a method similar to that described in *Masters et al.* [2009], we used a combination of magnetometer and ASPERA-IMA data to estimate the cross-sectional thickness of each HFA-candidate in the direction normal to the current sheet associated with each event. We assumed that the spacecraft is essentially stationary when compared to the supersonic flow of the solar wind. Next, we assumed that Cytherean HFAs are centered on the current sheet, and are "highly elongated", as described by *Koval et al.* [2005], who made multipoint observations of HFAs from the *INTERBALL-1* and *MAGION-4* spacecraft. Simulations by *Omidi and Sibeck* [2007] support this, showing HFAs which appear as tapering elongated fingers of hot plasma that extends along the tangential discontinuity and convects with the solar wind flow. It is important to note that with only a single spacecraft measurement, it was not possible to accurately determine the rate of expansion of the HFA, and thus, all sizes determined here represent the spatial extent of the HFA as observed by *Venus Express*.

First, using data from the Magnetometer, we measured how long it took for the core of each HFA to pass over the spacecraft (see third column, Table 2). Next, we calculated the orientation of the associated current sheet ($\hat{\mathbf{n}}$) using equation (2). Then, we obtained the local average solar wind velocity vector ($\hat{\mathbf{V}}_{sw}$) using observations by IMA, whose 2π field of view makes it ideal for this purpose. Using $\hat{\mathbf{V}}_{sw}$ and the duration, we calculated the size of the HFAs in the direction of the solar wind flow. Then, by taking $\hat{\mathbf{n}} \cdot \hat{\mathbf{V}}_{sw}$ and by using simple trigonometry, we estimated the thickness of the HFAs in the direction of $\hat{\mathbf{n}}$, as shown in the fourth column of Table 2 in both kilometers, and Venus Radii (R_V).

Figure 5 compares the relative sizes of HFAs at Venus, Earth, and Saturn. Figure 5d shows the physical sizes of HFAs (in kilometers) at each of the three planets. The diameter of each planet is also marked for scale. With thicknesses in the plane of the current sheet of ~2400 km (Event γ) to ~10,000 km (Event ζ), Cytherean HFAs tend to be physically smaller than their terrestrial counterparts. At Earth, where the solar wind obstacle is almost ten times larger, *Thomsen et al.* [1986] reports HFAs between 2551 km $\Rightarrow$ 44,008 km across. The monstrous Kronian HFA reported by *Masters et al.* [2009], at ~270,000 km across, dwarfs those observed in the inner solar system and is by far the largest HFA encountered to date. Thus, there appears to be some correlation between the size of the solar wind obstacle, and the size which an HFA can attain.

One possible explanation for this is that the larger the obstacle to the solar wind, the longer a discontinuity in the solar wind may remain attached, growing in response to additional reflected and energized solar wind plasma. The time taken (τ) for a current sheet to cross the bow shock from one side to the other (flank to flank) is given by equation (3).

$$\tau = \frac{2.\mathbb{BS}}{|\mathbf{V}_{sw}| \cos \theta_{\hat{\mathbf{n}}.\hat{\mathbf{x}}}} \tag{3}$$

where $\theta_{\hat{\mathbf{n}}.\hat{\mathbf{x}}}$ is the angle between the current sheet normal and the *x* axis, advecting with the solar wind at velocity $\mathbf{V}_{sw}$, and $\mathbb{BS}$ is the distance to the flanks from the center of the planet to the bow shock (in VSO coordinates, the radius of the bow shock where $x = 0$, not the subsolar standoff distance). Assuming $\theta_{\hat{\mathbf{n}}.\hat{\mathbf{x}}}$ ≈80°, and using typical dimensions of the bow shocks at each planet ($\mathbb{BS}_{Venus} = 7.9 \times 10^3$ km, $\mathbb{BS}_{Earth} = 1.4 \times 10^5$ km, and $\mathbb{BS}_{Saturn} = 1.5 \times 10^6$ km) and typical solar wind velocities ($|\mathbf{V}_{sw}|_{Venus}$

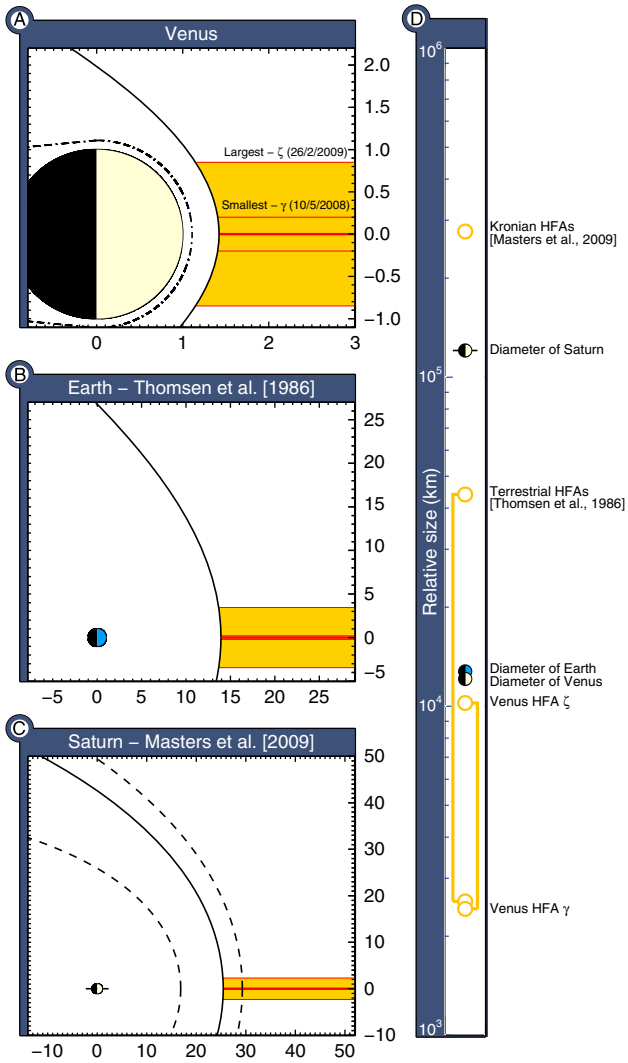

Figure 5. Comparing the relative sizes of HFAs to their parent magnetospheres, plotted to relative scale in planetary radii, but with the orientation of each HFA artificially shifted and rotated to lie along the planet/Sun line: (a) Venus (this study); (b) Earth according to *Thomsen et al.* [1986]; (c) Saturn according to *Masters et al.* [2009]. (d) Scale showing actual diameters (in kilometers) of Venus, Earth, and Saturn, and HFAs at each.

≈275 km/s, $|\mathbf{V}_{sw}|_{Earth}$ ≈390 km/s, and $|\mathbf{V}_{sw}|_{Saturn}$ ≈400 km/s), then to cross the bow shock from one flank to the other will take ≈5 min at Venus, ≈1 h at Earth, and ≈12 h at Saturn. Whilst this duration will vary greatly by $\theta_{\hat{\mathbf{n}}.\hat{\mathbf{s}}}$ (especially when close to 90°), they are qualitatively indicative that the larger the bow shock, the longer that an HFA has to grow, and thus the greater the size an HFA can attain. Thus, if and when HFAs are discovered in the foreshock of Jupiter, this would suggest that they will be the largest at any planet in the solar system. Another likely factor which drives the physical size of an HFA is the local ion gyroradius, which is ~50 km at Venus, ~80 km at Earth, and ~1000 km at Saturn (based on typical solar wind and IMF properties in the literature, e.g., *Slavin and Holzer* [1981]).

However, a more useful and meaningful comparison of scale can be made by depicting HFA sizes relative to those of the magnetospheres where they form. Figures 5a–5c show plots of the bow shocks of Venus (according to *Slavin et al.* [1980]), Earth [*Slavin and Holzer* 1981], and Saturn [*Arridge et al.*, 2006]. Each magnetosphere has been scaled to appear at approximately the same relative size on the plot. Units are in planetary radii. The largest and smallest HFAs reported at each planet have been plotted in gold with red borders. Note that they have been artificially rotated to lie along the Sun-planet line so that the relative scale of each can be more easily compared.

Although Cytherean HFAs (Figure 5a) are the smallest in absolute terms, they are in fact by far the largest when compared to the size of the local system. The ~1.7 R_V estimated diameter of Event ζ is ≈130% of the subsolar standoff distance of the bow shock (L ≈1.3 R_V [*Zhang et al.*, 1990]). For comparison, Saturn's seemingly titanic ~4.6R_S HFAs are actually far less dominating when compared to the overall size of the Kronian system (Figure 5c), being only 17% to 26% the subsolar standoff distance (17.7$R_S \leq L \leq$ 26.3R_S, depending on solar wind dynamic pressure [*Arridge et al.*, 2006]. The possible implications of this will be discussed later.

4.5. Motional Electric Fields

Past work indicates that inward pointing motional electric fields are required for HFA formation [*Schwartz et al.*, 2000]. *Collinson et al.* [2012a] found that for HFA β, motional electric fields pointed inward on both sides of the current sheet. However, this was just a single case study, and *Collinson et al.* [2012a] was unable to comment on whether or not this was common at Venus. Therefore, we have calculated the motional electric field vector before $\bar{\mathbf{E}}_{\text{pre}}$ and after $\bar{\mathbf{E}}_{\text{post}}$ according to equations (4) and (5).

$$\bar{\mathbf{E}}_{\text{pre}} = -\hat{\mathbf{v}}_{\text{sw}} \times \bar{\mathbf{B}}_{\text{pre}} \tag{4}$$

$$\bar{\mathbf{E}}_{\text{post}} = -\hat{\mathbf{v}}_{\text{sw}} \times \bar{\mathbf{B}}_{\text{post}} \tag{5}$$

We can confirm that in all cases, motional electric fields pointed inward toward the current sheet on at least one side, further supporting the theory that this is important for HFA formation. The fifth column of Table 2 lists on which side(s) the fields pointed inward: before, after, or on both sides.

4.6. Speed of Discontinuities

Another condition believed to be required for HFA formation is that the point at which the discontinuity intersects the bow shock must move along the bow shock at a sufficiently slow speed enabling the particles reflected by the bow shock to have an effect on the discontinuity. According to *Schwartz et al.* [2000], to fulfill this condition, the ratio of the transit velocity of the discontinuity (V_{tr}) to the gyrovelocity of the reflected ion (V_g) must be less than 1, as below in equation (6).

$$\left|\frac{V_{tr}}{V_g}\right| = \frac{\cos\theta_{\text{cs:sw}}}{2\,\cos\theta_{\text{bs:sw}}\,\sin\theta_n\,\sin\theta_{\text{cs:bs}}} < 1 \tag{6}$$

The results can be seen in the sixth column of Table 2, which lists the values both before and after the HFA. Note that the value listed for HFA β is an update from *Collinson et al.* [2012a], because actual IMA solar wind velocity vectors were used instead of a simple assumption of antisunward flow. In all but one case, this relationship holds true. However, in the case of event epsilon (ϵ), the speed ratios before and after are 1.36 and 3.11, respectively. On first inspection, this appears to be in contradiction to the current theory of HFA formation. However, we believe there is a simple explanation for this. From Figure 1, it can be seen that event ϵ was observed deep into the flanks of the Cytherian foreshock (≥90° longitude), and at a radial distance of ~2.8 R_V. Given that this is downstream, and event ϵ was ~0.6 R_V in spatial extent even at this relatively great distance from the planet (for an HFA), we posit that it is very likely that event ϵ has been swept into the flanks, and was observed shortly being swept off of the bow shock and into interplanetary space. It is therefore not unreasonable that this event violates the *Schwartz et al.* [2000] HFA formation criterion, because we do not believe that event ϵ formed in this location.

5. Summary

Using data from the *Venus Express* magnetometer, ion spectrometer, and electron spectrometer, and expanding on an initial case study of a single event [*Collinson et al.*, 2012a], we undertook a 3.06 sol (774 day) survey of Hot Flow Anomalies at the bow shock of the planet Venus (of which 2.53 sols (615 days) contained sufficient data, other orbits being rejected). Our findings have led us to the following conclusions:

1. HFAs are common at Venus, occurring on average approximately once or twice every 24 hours.
2. In every case motional electric fields pointed inward toward the discontinuity on at least one side, and the fields pointed inward on both sides in over half the cases, consistent with our understanding of HFA formation.

3. For all but one event, the velocity of the current sheet across the bow shock was calculated to be beneath the threshold for HFA formation described by *Schwartz et al.* [2000]. However, given that HFA ϵ violates this condition, we have shown that it is possible to observe HFAs with velocity ratios $V_{tr}/V_g > 1$, and that this condition breaks down as HFAs are swept across the flanks of Venus.
4. Electron density was enhanced in the compression regions of HFA ζ from $\approx$1 cm^{-3} to $\sim$2 $\rightarrow$ 2.5 cm^{-3}. Electron temperature increased from $\approx 2 \times 10^5 K$ to $8 \times 10^5 K$, consistent with observations of HFAs at the Earth and at Saturn.
5. Cytherian HFAs are physically smaller than their terrestrial or Kronian counterparts. However, they are very large when compared to the scale of the local (induced) magnetosphere, and occur very close to the planet.

On average, the frequency of HFAs at Venus was $\approx 1.2 \pm 0.8$ HFAs per day. Given the assumptions made and the very limited statistics available, this is consistent with the rate of $\approx$2 day^{-1} reported by *Facskó et al.* [2009], and thus, we conclude that HFAs occur at Venus at approximately the same frequency as at the Earth. Given that *Zhang et al.* [2008] reported that discontinuities in the solar wind are observed by the *Venus Express* magnetometer at a rate of approximately 3.5 day^{-1}, a subsequent rate of one or two HFAs per day seems plausible as a rough first-order estimation, given that not all discontinuities will generate an HFA.

All HFAs were observed when the solar wind was faster than average, and in two cases under exceptionally fast (> 600 km/s) conditions. These observations are consistent with the findings of *Facskó et al.* [2009, 2010] who reported that a requirement for HFA formation at Earth is a faster than average solar wind, although ideally more than seven events would be required for a rigorous examination of this condition at Venus. However, if this assumption is true, then this implies that just as at the Earth, HFAs can only form when the solar wind velocity is greater than a certain threshold. Our observations allow us to put an upper limit on this theoretical threshold of $\lessapprox$373 km/s, the slowest solar wind in which an HFA has been so far observed at Venus (HFA γ). An additional consequence of this would be that HFAs should be more common at solar maximum than at solar minimum (the dates arbitrarily chosen for this survey, 2008–2009, corresponded to the later).

Collinson et al. [2012a] speculated that; given the location of the bow shock and ionopause at Venus is known to be highly variable and dependent on solar wind dynamic pressure [*Brace et al.*, 1980; *Slavin et al.*, 1980; *Russell et al.*, 1988; *Martinecz et al.*, 2008; *Zhang et al.*, 1990; *Brace and Kliore*, 1991]; and that large pressure variations within HFAs drive large motions in Earth's Magnetopause [*Sibeck et al.*, 1999; *Jacobsen et al.*, 2009]; HFAs may play a very dominant role in the dynamics of the induced magnetosphere of Venus. In particular, it predicted HFAs drive significant motions in the bow shock and ionopause, and may possibly cause a disruption of orderly ionosheath flow.

This study has shown that HFAs are a common occurrence at Venus, that they are very large when compared to the size of the system (up to $\approx$130% of the subsolar standoff distance), and they occur very close to the planet (between 1.5 R_V and 3.0 R_V). This adds weight to our hypothesis, suggesting that HFAs are a very important mode of interaction between the solar wind and the Cytherean bow shock, and may drive widespread global effects throughout the induced magnetosphere and possibly into the ionosphere. However, it is not possible to directly study the effect of an HFA on the ionosphere with a single spacecraft, and therefore, this remains an open question for future studies or simulation.

Acknowledgments

This work was supported by an appointment to the NASA Postdoctoral Program at NASA Goddard Space-flight Center, administered by Oak Ridge Associated Universities through a contract with NASA. This work was also supported by UK STFC through a rolling grant to MSSL/UCL.

Masaki Fujimoto thanks the reviewers for their assistance in evaluating this paper.

References

Arridge, C. S., N. Achilleos, M. K. Dougherty, K. K. Khurana, and C. T. Russell (2006), Modeling the size and shape of Saturn's magnetopause with variable dynamic pressure, *J. Geophys. Res.*, *111*, A11227, doi:10.1029/2005JA011574.

Barabash, S., et al. (2007), The Analyser of Space Plasmas and Energetic Atoms (ASPERA-4) for the Venus Express mission, *Planet. Space Sci.*, *55*, 1772–1792.

Brace, L. H., and A. J. Kliore (1991), The structure of the Venus ionosphere, *Space Sci. Rev.*, *55*, 81–163.

Brace, L. H., R. F. Theis, W. R. Hoegy, J. H. Wolfe, J. D. Mihalov, C. T. Russell, R. C. Elphic, and A. F. Nagy (1980), The dynamic behavior of the Venus ionosphere in response to solar wind interactions, *J. Geophys. Res.*, *85*, 7663–7678.

Burgess, D. (1989), On the effect of a tangential discontinuity on ions specularly reflected at an oblique shock, *J. Geophys. Res.*, *94*, 472–478.

Collinson, G. A., D. O. Kataria, A. J. Coates, S. M. E. Tsang, C. S. Arridge, G. R. Lewis, R. A. Frahm, J. D. Winningham, and S. Barabash (2009), Electron optical study of the Venus Express ASPERA-4 Electron Spectrometer (ELS) top-hat electrostatic analyser, *Meas. Sci. Technol.*, *20*(5), 055204.

Collinson, G. A., et al. (2012a), Hot flow anomalies at Venus, *J. Geophys. Res.*, *117*, A04204, doi:10.1029/2011JA017277.

Collinson, G. A., et al. (2012b), The geometric factor of electrostatic plasma analyzers: A case study from the Fast Plasma Investigation for the Magnetospheric Multiscale mission, *Rev. Sci. Instrum.*, *83*(3), 033303.

Collinson, G. A., L. B. Wilson, III, D. G. Sibeck, N. Shane, T. L. Zhang, T. E. Moore, A. J. Coates, and S. Barabash (2012c), Short large-amplitude magnetic structures (SLAMS) at Venus, *J. Geophys. Res.*, *117*, A10221, doi:10.1029/2012JA017838.

Eastwood, J. P., D. G. Sibeck, J. A. Slavin, M. L. Goldstein, B. Lavraud, M. Sitnov, S. Imber, A. Balogh, E. A. Lucek, and I. Dandouras (2005), Observations of multiple X-line structure in the Earth's magnetotail current sheet: A Cluster case study, *Geophys. Res. Lett.*, *32*, L11105, doi:10.1029/2005GL022509.

Eastwood, J. P., et al. (2008), THEMIS observations of a hot flow anomaly: Solar wind, magnetosheath, and ground-based measurements, *Geophys. Res. Lett.*, *35*, L17S03, doi:10.1029/2008GL033475.

Facskó, G., K. Kecskeméty, G. Erdős, M. Tátrallyay, P. W. Daly, and I. Dandouras (2008), A statistical study of hot flow anomalies using Cluster data, *Adv. Space Res.*, *41*, 1286–1291.

Facskó, G., Z. Németh, G. Erdos, A. Kis, and I. Dandouras (2009), A global study of hot flow anomalies using Cluster multi-spacecraft measurements, *Ann. Geophys.*, *27*, 2057–2076.

Facskó, G., J. G. Trotignon, I. Dandouras, E. A. Lucek, and P. W. Daly (2010), Study of hot flow anomalies using Cluster multi-spacecraft measurements, *Adv. Space Res.*, *45*, 541–552.

Gary, S. P. (1991), Electromagnetic ion/ion instabilities and their consequences in space plasmas—A review, *Space Sci. Rev.*, *56*, 373–415.

Hudson, P. D. (1970), Discontinuities in an anisotropic plasma and their identification in the solar wind, *Planet. Space Sci.*, *18*, 1611–1622.

Jacobsen, K. S., et al. (2009), THEMIS observations of extreme magnetopause motion caused by a hot flow anomaly, *J. Geophys. Res.*, *114*, A08210, doi:10.1029/2008JA013873.

Koval, A., J. Šafránková, and Z. Němeček (2005), A study of particle flows in hot flow anomalies, *Planet. Space Sci.*, *53*, 41–52, doi:10.1016/j.pss.2004.09.027.

Lucek, E. A., T. S. Horbury, A. Balogh, I. Dandouras, and H. Rème (2004), Cluster observations of hot flow anomalies, *J. Geophys. Res.*, *109*, A06207, doi:10.1029/2003JA010016.

Martinecz, C., et al. (2008), Location of the bow shock and ion composition boundaries at Venus Initial determinations from Venus Express ASPERA-4, *Planet. Space Sci.*, *56*(6), 780–784.

Masters, A., C. S. Arridge, M. K. Dougherty, C. Bertucci, L. Billingham, S. J. Schwartz, C. M. Jackman, Z. Bebesi, A. J. Coates, and M. F. Thomsen (2008), Cassini encounters with hot flow anomaly-like phenomena at Saturn's bow shock, *Geophys. Res. Lett.*, *35*, L02202, doi:10.1029/2007GL032371.

Masters, A., et al. (2009), Hot flow anomalies at Saturn's bow shock, *J. Geophys. Res.*, *114*, A08217, doi:10.1029/2009JA014112.

Øieroset, M., D. L. Mitchell, T. D. Phan, R. P. Lin, and M. H. Acuña (2001), Hot diamagnetic cavities upstream of the Martian bow shock, *Geophys. Res. Lett.*, *28*, 887–890.

Omidi, N., and D. G. Sibeck (2007), Formation of hot flow anomalies and solitary shocks, *J. Geophys. Res.*, *112*, A01203, doi:10.1029/2006JA011663.

Omidi, N., H. Zhang, D. Sibeck, and D. Turner (2013), Spontaneous hot flow anomalies at quasi-parallel shocks: 2. Hybrid simulations, *J. Geophys. Res. Space Physics*, *118*, 173–180, doi:10.1029/2012JA018099.

Onsager, T. G., M. F. Thomsen, J. T. Gosling, and S. J. Bame (1990), Observational test of a hot flow anomaly formation mechanism, *J. Geophys. Res.*, *95*, 11,967–11,974.

Paschmann, G., G. Haerendel, N. Sckopke, E. Moebius, and H. Luehr (1988), Three-dimensional plasma structures with anomalous flow directions near the Earth's bow shock, *J. Geophys. Res.*, *93*, 11,279–11294.

Russell, C. T., E. Chou, J. G. Luhmann, P. Gazis, L. H. Brace, and W. R. Hoegy (1988), Solar and interplanetary control of the location of the Venus bow shock, *J. Geophys. Res.*, *93*, 5461–5469.

Schwartz, S. J. (1995), Hot flow anomalies near the Earth's bow shock, *Adv. Space Res.*, *15*, 107–116.

Schwartz, S. J., C. P. Chaloner, D. S. Hall, P. J. Christiansen, and A. D. Johnstone (1985), An active current sheet in the solar wind, *Nature*, *318*, 269–271.

Schwartz, S. J., R. L. Kessel, C. C. Brown, L. J. C. Woolliscroft, and M. W. Dunlop (1988), Active current sheets near the Earth's bow shock, *J. Geophys. Res.*, *931*, 11,295–11,310.

Schwartz, S. J., G. Paschmann, N. Sckopke, T. M. Bauer, M. Dunlop, A. N. Fazakerley, and M. F. Thomsen (2000), Conditions for the formation of hot flow anomalies at Earth's bow shock, *J. Geophys. Res.*, *105*, 12,639–12,650.

Sibeck, D. G., N. L. Borodkova, G. N. Zastenker, S. A. Romanov, and J.-A. Sauvaud (1998), Gross deformation of the dayside magnetopause, *Geophys. Res. Lett.*, *25*, 453–456.

Sibeck, D. G., et al. (1999), Comprehensive study of the magnetospheric response to a hot flow anomaly, *J. Geophys. Res.*, *104*, 4577–4594.

Slavin, J. A., and R. E. Holzer (1981), Solar wind flow about the terrestrial planets. I—Modeling bow shock position and shape, *J. Geophys. Res.*, *86*, 11,401–11,418.

Slavin, J. A., R. C. Elphic, C. T. Russell, F. L. Scarf, J. H. Wolfe, J. D. Mihalov, D. S. Intriligator, L. H. Brace, H. A. Taylor, and R. E. Daniell (1980), The solar wind interaction with Venus—Pioneer Venus observations of bow shock location and structure, *J. Geophys. Res.*, *85*, 7625–7641.

Slavin, J. A., et al. (2009), MESSENGER and Venus Express observations of the solar wind interaction with Venus, *Geophys. Res. Lett.*, *36*, L09106, doi:10.1029/2009GL037876.

Svedhem, H., et al. (2007), Venus Express—The first European mission to Venus, *Planet. Space Sci.*, *55*, 1636–1652.

Thomas, V. A., D. Winske, M. F. Thomsen, and T. G. Onsager (1991), Hybrid simulation of the formation of a hot flow anomaly, *J. Geophys. Res.*, *96*, 11,625–11,632.

Thomsen, M. F., J. T. Gosling, S. A. Fuselier, S. J. Bame, and C. T. Russell (1986), Hot, diamagnetic cavities upstream from the Earth's bow shock, *J. Geophys. Res.*, *91*, 2961–2973.

Thomsen, M. F., J. T. Gosling, S. J. Bame, K. B. Quest, and C. T. Russell (1988), On the origin of hot diamagnetic cavities near the Earth's bow shock, *J. Geophys. Res.*, *93*, 11,311–11,325.

Thomsen, M. F., V. A. Thomas, D. Winske, J. T. Gosling, M. H. Farris, and C. T. Russell (1993), Observational test of hot flow anomaly formation by the interaction of a magnetic discontinuity with the bow shock, *98*, 15,319–15,330, doi:10.1029/93JA00792.

Titov, D. V., et al. (2006), Venus Express science planning, *Planet. Space Sci.*, *54*, 1279–1297.

Tjulin, A., E. A. Lucek, and I. Dandouras (2008), Wave activity inside hot flow anomaly cavities, *J. Geophys. Res.*, *113*, A08113, doi:10.1029/2008JA013333.

Wang, S., Q. Zong, and H. Zhang (2013), Cluster observations of hot flow anomalies with large flow deflections: 2. Bow shock geometry at HFA edges, *J. Geophys. Res. Space Physics*, *118*, 418–433, doi:10.1029/2012JA018204.

Zhang, H., D. G. Sibeck, Q.-G. Zong, S. P. Gary, J. P. McFadden, D. Larson, K.-H. Glassmeier, and V. Angelopoulos (2010), Time History of Events and Macroscale Interactions during Substorms observations of a series of hot flow anomaly events, *J. Geophys. Res.*, *115*, A12235, doi:10.1029/2009JA015180.

Zhang, H., D. G. Sibeck, Q.-G. Zong, N. Omidi, D. Turner, and L. B. N. Clausen (2013), Spontaneous hot flow anomalies at quasi-parallel shocks: 1. observations, *J. Geophys. Res. Space Physics*, *118*, 3357–3363, doi:10.1002/jgra.50376.

Zhang, T.-L., J. G. Luhmann, and C. T. Russell (1990), The solar cycle dependence of the location and shape of the Venus bow shock, *J. Geophys. Res.*, *95*, 14,961–14,967.

Zhang, T. L., et al. (2006), Magnetic field investigation of the Venus plasma environment: Expected new results from Venus Express, *Planet. Space Sci.*, *54*, 1336–1343.

Zhang, T. L., et al. (2008), Behavior of current sheets at directional magnetic discontinuities in the solar wind at 0.72 AU, *Geophys. Res. Lett.*, *352*, L24102, doi:10.1029/2008GL036120.